ESO observing programme: *Looking into the faintest with MUSE (LEWIS)*

Abstract

Looking into the faintEst WIth MUSE (LEWIS) is an ESO large observing programme approved in 2021 (P.I. E. Iodice, Prog.ID 108.222P) which was granted 133.5 hours at the Multi Unit Spectroscopic Explorer (MUSE, Bacon et al. 2010) at the VLT. LEWIS is the first homogeneous integral-field (IF) follow-up spectroscopic survey of 30 extreme low surface brightness (LSB) galaxies in the Hydra I cluster of galaxies. The majority of LSB galaxies in the sample (22 in total) are ultra-diffuse galaxies (UDGs). The project description, sample selection, and preliminary results have been published in LEWIS Paper I, by Iodice et al. 2023. For a sample of UDGs in the galaxy cluster, the new IF spectroscopic data acquired with the LEWIS project enable us to map for the first time

1. the 2D stellar kinematics;
2. the stellar population;
3. the globular clusters (GCs) content and their specific frequency.

Therefore, the LEWIS data allow us to address the following science goals, which are the main debated issues on the nature of UDGs:

- ***DM content in each UDG*** of the sample through dynamical mass estimates from stellar kinematics. Results are published in **LEWIS Paper II, by Buttitta et al. 2025**;
- ***The star formation history of UDGs*** from SED fitting of their integrated spectra, to study the evolutionary link between the UDGs and dwarf galaxies through a comparison of their stellar population and structural properties. Results are published in **LEWIS Papers III and V, by Hartke et al. 2025 and Doll et al. 2025**;
- The spectroscopic confirmation of GC candidates around UDGs can improve their S_N ***estimates***, which in turn will put on a firmer basis the discussion about possible overdensities of GCs around some UDGs and the relation to the host galaxy DM content. Results are published in **LEWIS Paper IV, by Mirabile et al. 2025**.

Overview of observations

The MUSE observations for the LEWIS project were carried out in service mode between December 2021 and March 2025 under the program ID 108.222P. MUSE is used in Wide Field Mode without adaptive optics, providing a field of view (FoV) of 1×1 arcmin^2, with a spatial sampling of 0.2×0.2 arcsec^2. The nominal wavelength range of MUSE is from 4800 to 9300 Å, with a spectral resolution (FWHM) that varies from 2.74 Å (69 km/s) at 5000 Å to 2.54 Å (46 km/s) at 7000 Å (Bacon et al. 2017). Since galaxies in the LEWIS sample span a wide range of values of effective surface brightness $25 \leq \mu_e \leq 27$ mag/arcsec^2, the total integration time adopted for each target was set by a required limiting magnitude $\mu_{lim} = \mu_e$ and a minimum signal-to-noise ratio SNR=7 in a spectral bin (= 2.51Å) of 2×2 pixels for the brighter targets and 5×5 pixels for the fainter targets. Given that, the total integration times range from 2 hours for galaxies with $\mu_e \simeq 25$ mag/arcsec^2 up to ~6 hours for targets with $\mu_e \simeq 27$ mag/arcsec^2. The total execution time for the DR1 targets is reported in Table 1. A dither of a few arcseconds and a rotation by 90 degrees were applied to the single exposures to minimize the signature of the 24 MUSE slicers on the field of view. Since all LEWIS targets are less extended than the MUSE FoV (see also Fig.1 and Fig.2), the sky has been evaluated directly on the science frames, as described in the following section. The observations were done in good seeing conditions with a median FWHM = 0.9 arcsec.

Release Content

The first data release (DR1) of the LEWIS project includes five galaxies of the sample, which are listed in Table 1 and shown in Fig.1 and Fig.2. For these UDGs, the data analysis on stellar kinematics, stellar population, and GCs content was completed and published in the first five papers of the LEWIS series. The reduced data of all remaining targets of the sample will be released in a forthcoming DR.

The DR1 consists of a datacube file and a white-light image per each galaxy, obtained from the improved data reduction we performed on LEWIS data (see section on the data reduction). For UDG32, we additionally released the not-cleaned reduced cube, which was effectively used to derive the stellar population analysis (see Hartke et al., 2025). In total, DR1 contains 6 datacube files and 6 white-light images.

The total data volume is ~8.9 GB. The target list and their basic properties from the literature are provided in Table 1. The spectral range covered by the MUSE cubes for all five galaxies in DR1 is 4000 - 9000 Å.

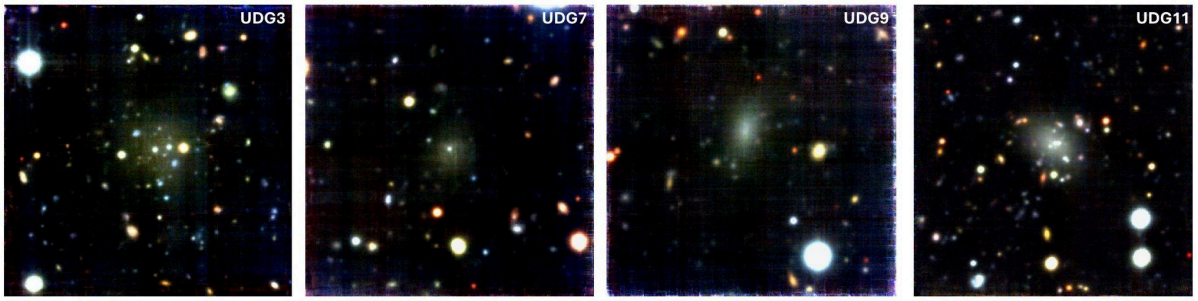

Fig. 1: Colour-composite images of four of the five galaxies of the DR1 of the LEWIS data: UDG3, UDG7, UDG9, and UDG11.

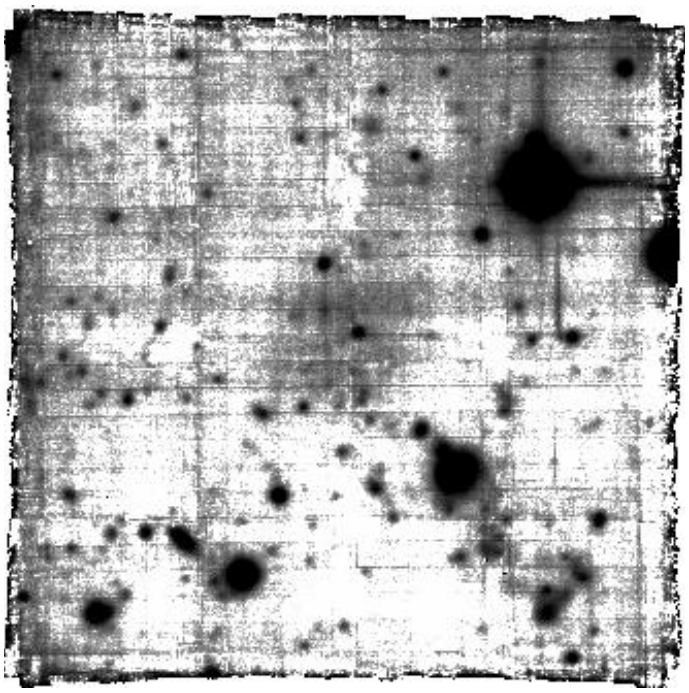

Fig. 2: White-light image of UDG 32, obtained from the cleaned reduced MUSE datacube.

Table 1: Target list and properties of the LEWIS DR1.

Target name (1)	R.A. [J2000] (2)	DEC [J2000] (3)	Exec. time [hrs] (4)	Observing date (5)	V_{sys} [km/s] (6)	μ_0 [mag/arcsec^2] (7)	R_{eff} [kpc] (8)	S/N (9)	mag_{lim} [mag] (10)
UDG3	10:36:58.63	-27:08:10.21	5.0	Feb 2023; Mar 2025	3611 ± 14	25.2 ± 0.2	1.88 ± 0.12	15	25.5
UDG7	10:36:37.16	-27:22:54.93	4.2	Jan-Feb-Mar 2023	4126 ± 5	24.4 ± 0.4	1.66 ± 0.12	17	25.2
UDG9	10:37:22.85	-27:36:02.80	3.9	Dec 2021; Jan-Mar 2022	4269 ± 4	24.2 ± 0.2	3.46 ± 0.12	19	25.0
UDG11	10:34:59.55	-27:25:37.95	4.6	Jan-Mar 2023	3507 ± 3	24.4 ± 0.1	1.66 ± 0.12	19	26.6
UDG32	10:37:04.20	-27:42:53.92	5.0	Feb-Mar 2022	3080 ± 120	26.2 ± 1.0	3.80 ± 1.00	3*	24.7

Notes: In column 1 is given the target name (from Iodice et al. 2023). In columns 2 and 3, the J2000 celestial coordinates are listed. Columns from 4 to 5 indicate the total execution time on the target and the observing date, respectively. Column 6 lists the systemic radial velocity derived from the MUSE data. In Columns 7 and 8 are listed the central surface brightness (μ_0) and effective radius (R_e), derived from the g-band optical data (Iodice et al. 2020). Columns from 9 to 10 indicate the average signal-to-noise (S/N) ratio of the stacked spectra inside 1 R_{eff} and the limiting magnitude of the MUSE cube in the AB system.
*: the value corresponds to the S/N of the stacked spectrum of an aperture as close as possible to UDG 32 center, not containing the strong gaseous emission of filaments from nearby galaxy NGC 3314A

Release Notes

Data Reduction and Calibration

The LEWIS data were reduced using the MUSE pipeline routine (Weilbacher et al. 2020), running in the ESOREFLEX environment (Freudling et al. 2013).

The steps of the standard data reduction included bias and overscan subtraction, lamp flat-fielding correction, wavelength calibration, determination of the line spread function (LSF), illumination correction, sky-background subtraction, and flux calibration. For each object, the different exposures were aligned and combined to produce the final combined datacube. Since the resulting sky-subtracted datacube was characterised by the contamination of sky residuals, the datacubes were cleaned by applying the Zurich Atmospheric Purge algorithm (ZAP, Soto et al. 2016).
As described in LEWIS' papers I, II, and III (Iodice et al. 2023, Buttitta et al. 2025, Hartke et al. 2025), we improved the standard data reduction to reduce sky-background and flat-fielding residuals and improved the quality of the data. We have added a few changes to a modified ESOREFLEX workflow, as described below and shown in Fig.3 (left panel).

Custom mask - For each sample galaxy, we extracted the white-light image by collapsing the datacube resulting from a first standard reduction along the wavelength direction. We built a custom mask, detecting and masking all the possible light contamination from the foreground, background, and spurious sources, including the contribution of the target. All sources were detected using the deep images available for this cluster (Iodice et al. 2020b, La Marca et al. 2022b).

This mask improved the sky-background estimate, and it was directly injected in the ESOREFLEX workflow with additional parameters $SkyFr_1$=0.75 and $SkyFr_2$=0., where $SkyFr_1$ and $SkyFr_2$ are the fractions of spaxels in the sky image and scientific image used to evaluate the sky background, respectively.

Normalisation of the exposures - We adapted a two-step approach to normalise the flux variations across the FOV and between exposures. To reduce slice-to-slice flux variations, we used for each exposure the *autocalibration=deepfield* algorithm developed for the MUSE deep fields, which calculates calibration factors that were applied to each pixel table. When combining the exposures into the final datacube, we also accounted for flux variations of different exposures (e.g., due to different observing conditions and sky levels) with a multiplicative correction. Some of the galaxies in LEWIS presented a spectral discontinuity caused by the normalization of the flux in the several MUSE slices performed with option *autocalibration=deepfield* (see Weilbacher et al. 2020 for a description) This occurs for UDG3, UDG7 and UDG9. After inspecting the quality of the stacked spectrum obtained from the cleaned datacube, we performed again the normalization step with *autocalibration=none* to correct and solve the discontinuity.

ZAP with custom mask - We used the custom mask in the ZAP routine to improve the detection of the sky-background filtering, all the light contributions in the FOV. In addition, we realised that the automatic application of ZAP partially removed the flux of the galaxy target. Thus, we tested different combinations of parameters to minimise the subtraction of the signal from the target. We used *cfwidthSP* between [30,50] and *cfwidthSVD* between [10,30] (see discussion in Soto et al. 2016), where *cfwidthSP* is the window size for the continuum filter used to remove the continuum features for calculating the eigenvalues per spectrum, and *cfwidthSVD* is the window size for the continuum filter for the SVD computation.

Notes on the special case: UDG32

The data reduction of UDG 32 followed the same general philosophy as that of the other UDGs in the sample, with two notable exceptions (see Fig. 3, right panel), as discussed in Hartke et al. (2025). Due to the presence of a diffuse gaseous filament that is ram-pressure stripped from the nearby Hydra I cluster galaxy NGC 3314A, constructing a mask from the white-light image was not sufficient. Using the 'standard' LEWIS data reduction resulted in data cubes with 'fake' absorption lines, as the redshifted Hα line at ~6630 Å was misinterpreted as OH sky lines. We therefore constructed a second mask from a 20 Å-wide pseudo-narrow image centred on the Hα emission, and, like for the other UDGs, also masked the central ⅓ effective radii. Since this additional mask led to 50% of the field of view being masked, we merged the per-exposure autocalibration tables into a single one, applying the algorithm provided by the MPDAF package (Bacon et al., 2016; Piqueras et al., 2017) following the recommendation by Weilbacher et al. (2021). Having applied the new user-defined autocalibration table to each pixel table, we then combined the pixel tables with a multiplicative correction as described earlier. Before running ZAP (Soto et al., 2016) to obtain the cleaned datacube, we updated both the white-light and Hα-based mask based on the newly reduced data cube. We ZAPped the data with the default continuum filter width ***(cfwidthSP=300)*** and best-fit number of eigenspectra ***(nevals=91)***.

While we mainly used the cleaned datacube for the analysis in Hartke et al. (2025), we also released the reduced (i.e. not ZAPped) datacube, as we used it to test the robustness of our results. However, we found no significant difference in the derived stellar kinematics and population parameters between the reduced and cleaned cubes, as we restricted the analysis to the optical wavelength regime (< 7100 Å).

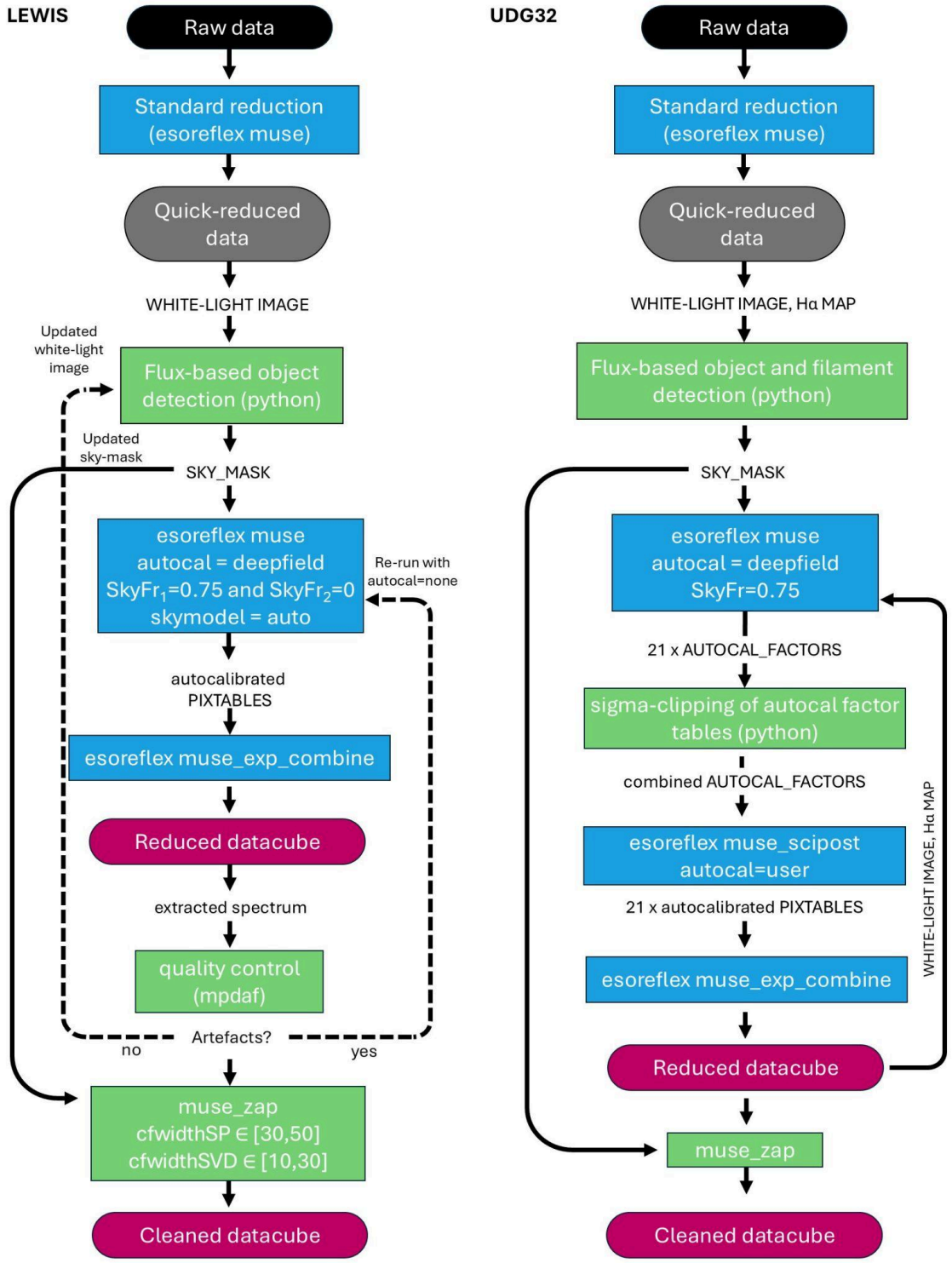

Fig.3: Data reduction flowchart sketching the process of obtaining the cleaned data cube from raw data for LEWIS galaxies (right panel) and UDG32 (left panel). ESO reflex and esorex pipeline processes are shown in blue and auxiliary python routines in green boxes. Readapted from Hartke at al. 2025.

Data quality

Spectral resolution - We investigated possible systematic variations and determined the MUSE line-spread function (LSF) of the LEWIS data applying the following procedure. For each exposure, we extracted 5 spectra of the sky background in a circular aperture of a radius of 15 pixels in different regions across the FOV. We selected a set of 14 not-blended sky emission lines and measured their FWHM by performing an interpolation with a second order polynomial. We finally estimated the LSF by calculating the weighted mean average of the FWHMs across the wavelength range and compared the resulting LSF with those obtained from the different exposures and from the whole combined datacube. After confirming the agreement between the LSF measured from the single exposures and the combined datacube, we derived the LSF directly from the combined cubes for all the UDGs in the LEWIS sample. We found similar trends for datasets belonging to different UDGs. This means that the instrumental LSF is not affected by the chosen observing strategy or by the nature of the target itself. We finally refined the estimation of the MUSE LSF by fitting data with a polynomial function of grade equal to 2, as done in Bacon et al. (2017). From the best-fitting polynomial function, we found:

$$FWHM(\lambda) = 1.185 \cdot 10^{-8}\,\lambda^2 - 1.916 \cdot 10^{-4}\,\lambda + 3.397$$

In the optical wavelength range, it is reasonable to adopt an average constant value for the LSF of FWHM[4800-7000] = 2.69Å (see also Buttitta et al., 2025).

Depth of observations - In the header of each datacube is reported the value of the magnitude limit reached on the combined exposures under the keyword ABMAGLIM (Col 10 in Table 1). The value is calculated using the recipe hdrldemo_maglim, available at https://ftp.eso.org/pub/dfs/pipelines/hdrl/ and corresponds to the AB magnitude of a point-like source with flux equal to 5σ of the background and a point-spread function equal to the average seeing measured on the combined exposure (keyword SKY_RES).

Signal-to-noise - The values of the S/N reported in Table 1 correspond to the average S/N of a stacked spectrum extracted from an elliptical aperture centred on the galaxy center, with semi-major axis equal to R_{eff} and with ellipticity and position angle from isophotal analysis carried out on white-light image (see Buttitta et al., 2025 for details). This is the stacked spectrum used to carry out the analysis of integrated stellar kinematics and stellar population properties. The S/N is computed using the following function: ***der_SNR.py*** (www.stecf.org/software/ASTROsoft/DER_SNR/) on stacked spectrum after masking all the noisy regions in the spectral wavelength range 4800-7000 Å or 4800-9000Å when the Calcium triplet is feasible (see details in Buttitta et al., 2025).

Known issues

None

Data Format

Files Types

The data for each target listed in Table 1 consists of a datacube and the white-light image computed as an average along the datacube spectral direction. Each file, either datacube or associated image, is in FITS format. For the datacube, the basic information is stored in the primary header of the file, which is followed by a DATA extension. For the white-light image, the basic information and data are stored in the primary extension. Error extensions are not included in the release.

Acknowledgements

The LEWIS scientific publications based on DR1 data are:

1. Doll G., Buttitta C., Iodice E. et al. 2025, A&A, in press: *Looking into the faintEst WIth MUSE (LEWIS): Exploring the nature of ultra-diffuse galaxies in the Hydra I cluster. V. Integrated stellar population properties*

2. Mirabile M., Cantiello M., Rejkuba M. et al. 2025, A&A, in press: *Looking into the faintEst WIth MUSE (LEWIS): Exploring the nature of ultra-diffuse galaxies in the Hydra-I cluster IV. A study of the Globular Cluster population in four UDGs.*

3. Hartke J., Iodice E., Gullieuszik M. et al. 2025, A&A 695, 91: *Looking into the faintEst WIth MUSE (LEWIS): Exploring the nature of ultra-diffuse galaxies in the Hydra I cluster. III. Untangling UDG32 from the stripped filaments of NGC3314A in the Hydra I cluster*

4. Buttitta C., Iodice E., Doll G. et al., 2025, A&A 694, A276: *Looking into the faintEst WIth MUSE (LEWIS): Exploring the nature of ultra-diffuse galaxies in the Hydra-I cluster. II. Stellar kinematics and dynamical masses*

5. Iodice E., Hilker M., Doll G. et al., 2023, A&A 665, 105: *Looking into the faintEst WIth MUSE (LEWIS): Exploring the nature of ultra-diffuse galaxies in the Hydra-I cluster. I. Project description and preliminary results*

6. Forbes D., Gannon J., Iodice E. et al., 2023, MNRAS Letter 525, 93: *Ultra diffuse galaxies in the Hydra I cluster from the LEWIS Project: Phase-Space distribution and globular cluster richness*

We acknowledge support from the following funding grants:

- INAF GO funding grant 2022-2023 (PI E. Iodice, INAF)
- INAF Large funding grant 2022-2023 (PI L. Hunt, INAF)
- Italian Ministry for Education, University and Research (MIUR) grant PRIN 2022 2022383WFT "SUNRISE", CUP C53D23000850006 (PI E. Iodice, INAF)
- visitor and mobility programme of the Finnish Centre for Astronomy with ESO (FINCA).

We acknowledge support from Lodovico Coccato of ESO during the preparation of data products for this DR1.
We wish to acknowledge CSC – IT Center for Science, Finland, for computational resources.
Data products of DR1 are created from observations collected at the European Organisation for Astronomical Research in the Southern Hemisphere under the following ESO programme: **108.222P.**
Any publication making use of this data, whether obtained from the ESO archive or via third parties, must include the following acknowledgment:
"*Based on data products created from observations collected at the European Organisation for Astronomical Research in the Southern Hemisphere under ESO programme: 108.222P.*"
Publications making use of data must include the following statement in a footnote or in the acknowledgement:
Based on data obtained from the ESO Science Archive Facility with DOI: https://doi.org/10.18727/archive/104[1].